Vol. 17, No. 2 (2018) 693-705
Revista Mexicana de Ingeniería Química

EFFECT OF SILICA SOURCE ON THE SYNTHESIS AND PROPERTIES OF POLYSULFONE/SILICA COMPOSITE MEMBRANES FOR GAS SEPARATION

EFECTO DE LA FUENTE DE SÍLICE EN LA SÍNTESIS Y PROPIEDADES DE MEMBRANAS COMPUESTAS DE POLISULFONA/SÍLICE PARA SEPARACIÓN DE GASES

G. Castruita-de León[1]*, H.I. Meléndez-Ortiz[1], Y.A. Perera-Mercado[2], J.A. Mercado-Silva[3], L.A. García-Cerda[3], A. de J. Montes-Luna[3], S.P. García-Rodríguez[3]

[1] *CONACYT-Centro de Investigación en Química Aplicada; Blvd. Enrique Reyna Hermosillo # 140, CP 25294, Saltillo, Coahuila, México.*

[2] *West Houston Center for Science & Engineering (WHC) at the Houston Community College System (HCCS). 2811 Hayes Road, Houston, Texas, U.S.*

[3] *Centro de Investigación en Química Aplicada; Blvd. Enrique Reyna Hermosillo # 140, CP 25294, Saltillo, Coahuila, México*

Received September 19, 2017; Accepted February 26, 2018

Abstract

This work reports the synthesis in-situ of silica particles inside a polysulfone matrix by the sol-gel method in acidic medium using different polymerization inorganic precursors: tetraethylorthosilicate (TEOS), 3-aminopropyltriethoxysilane (APTES) and mixture of them. The effect of the type of inorganic precursor on the formation of silica particles was studied. Composite membranes were prepared by casting technique from these organic-inorganic materials. These membranes were characterized by X-ray diffraction (XRD), infrared spectroscopy (FTIR), differential scanning calorimetry (DSC) and thermogravimetric analysis (TGA). The morphology, particle size and particle-polymer interaction were studied by scanning electron microscopy (SEM). Additionally, a semi-quantitative chemical analysis by energy dispersive X-ray spectroscopy (EDX) showed the chemical composition of the composite membranes. Type and concentration of silica precursor affected the morphology, particle size and distribution of silica in the composite membranes. Composite membranes without interfacial voids were obtained from APTES at 25 wt%. Initial studies about the gas separation properties of CO_2/CH_4 gas mixture revealed an improvement on the CO_2 permeability of composite membrane comprising silica particles synthesized from APTES in comparison with the polymeric membrane.

Keywords: silica, sol-gel, polysulfone, composite membrane, gas separation.

Resumen

En este trabajo se reporta la síntesis in-situ de partículas de sílice dentro de una matriz de polisulfona mediante el método sol-gel en medio ácido usando diferentes precursores inorgánicos de polimerización: tetraetilortosilicato (TEOS), 3-aminopropiltrietoxisilano (APTES) y mezcla de ambos. Se estudió el efecto del tipo de precursor inorgánico en la formación de las partículas de sílice. Las membranas compuestas se prepararon por evaporación del disolvente a partir de los materiales orgánico-inorgánico. Estas membranas se caracterizaron por difracción de rayos X (XRD), espectroscopía de infrarrojo (FTIR), calorimetría diferencial de barrido (DSC) y análisis termogravimétrico (TGA). La morfología, tamaño de partícula y la interacción partícula-polímero se estudiaron por microscopia electrónica de barrido (SEM). Adicionalmente, el análisis químico semicuantitativo mediante espectroscopía de energía dispersiva de rayos X (EDX) mostró la composición química de las membranas compuestas. El tipo y la concentración del precursor de la sílice afectaron la morfología, el tamaño de partícula y la distribución de la sílice en las membranas compuestas. Las membranas compuestas que fueron obtenidas a partir de APTES al 25% no mostraron huecos interfaciales. Estudios iniciales de las propiedades de separación de una mezcla CO_2/CH_4 revelaron el mejoramiento de la permeabilidad de CO_2 de las membranas compuestas que contienen partículas de sílice sintetizadas a partir de APTES en comparación con la membrana polimérica.

Palabras clave: sílice, sol-gel, polisulfona, membrana compuesta, separación de gases.

* *Corresponding author. E-mail*: griselda.castruita@ciqa.edu.mx
Tel. +52 844 4389830 x1013; Fax: +52 844 4389839
doi: 10.24275/10.24275/uam/izt/dcbi/revmexingquim/2018v17n2/Castruita
issn-e: 2395-8472

1 Introduction

The inorganic-organic composites have been extensively studied during the last decades. The incorporation of an inorganic component into a polymer matrix results in a hybrid material which exhibits better specific properties than both organic matrix and inorganic material by separate (Xu *et al*., 2009; Pérez-Escobedo *et al*., 2016). These materials can be used in attractive applications such as catalysis (Hasik *et al*.,2009; Starlet *et al*., 2012), biomaterials (Wei *et al*., 2007; Vallés-Lluch *et al*., 2010), sensors (Kang *et al*., (2010); Zeng *et al*., 2007), coatings (Torrey *et al*., 2008; Armstrong *et al*. 2012), and membranes (Jomekian *et al*., 2011; Sadeghi *et al*., 2011). For instance, the use of polymeric-inorganic composites has been successfully employed to enhance the performance of membranes for gas separation (Lua *et al*., 2013; Khosravi *et al*., 2014).

The organic-inorganic composite membranes have been commonly obtained from three different ways. In the first way, an inorganic filler previously prepared is mixed with a polymeric solution and dispersed by stirring and ultrasonic treatment (Mahajan *et al*., 2002). Nevertheless, critical factors as the interface voids derived from a poor compatibility between both phases (Chung *et al*., 2007) and the difficulty to eliminate the particle agglomeration have often been reported as the main disadvantages of this method (Jomekian *et al*., 2011). In the second case, the organic monomers are polymerized at the surface of functionalized inorganic particles giving a covalent junction each other (Babanzadeh *et al*., 2012). The last and more convenient way involves the in-situ growth of the inorganic material inside the organic continuous phase either in monomeric or polymeric solution, i.e., the sol-gel method. In this method, the inorganic precursor is hydrolyzed and condensed under acid or basic conditions without formation of a covalent junction with the polymer (Kim *et al*. 2001). In addition, this technique is very useful for the preparation of films, coatings and, membranes by casting. The sol-gel method offers better control on the connectivity between inorganic-organic phases giving more homogeneous hybrid composite, morphology, particle size, and less phase segregation (Xu *et al*., 2009; Zarazua-Aguilar *et al*., 2017).

In order to achieve this aim, the adhesion among both components can be enhanced by the introduction of functional groups on the structure of the inorganic material which could provide either a covalent attached or physical interactions (e.g. hydrogen bonds or Van der Waals forces) with the functionalities on the polymeric matrix, improving the interface compatibility and getting a well-dispersed inorganic network (Zhuang *et al*., 2014; Wu *et al*., 2013). Functional groups such as carbonyl, hydroxyl, ether or amine on the polymer structure can interact physically with the functionalities of the inorganic phase. This interaction could contribute to obtain better dispersion of the inorganic material, the improvement in the thermal stability, mechanical properties, and permselectivity properties of the composite membranes (Naghsh *et al*., 2012; Ghadimi *et al*., 2014).

Silica has been one of the most important inorganic compounds used on composite membranes for application in gas separation due to its attractive thermal and sorption properties (Chew *et al*., 2010; Hasebe *et al*., 2017). Tetraethylorthosilicate (TEOS) has been the main source for preparing silica particles. Nevertheless, the introduction of amino groups within the silica framework by using an organosilane has been used to enhance inorganic-polymeric compatibility and improve the interactions with CO_2 facilitating its adsorption process (Gil *et al*., 2011; Basu *et al*., 2010, Castruita *et al*., 2015, Sánchez-Ruiz *et al*., 2018). Romero *et al*. 2013, reported the improvement on the thermal, morphological and mechanical properties of hybrid polyetherimide-silica membranes by using an organoaminosilane as coupling agent. The increase on Young's modulus is attributed to the higher interaction between organic and inorganic phase given by the coupling agent. On the other hand, the relationship between polymer-filler interfaces of polyvinylamine-based composite membranes containing silica and other post-grafted amino-modified nanofillers has been reported by Wang *et al*. 2015. They suggested that the surface modification of fillers could improve the interface compatibility. Despite several researches have studied the incorporation of inorganic fillers in membranes in order to improve the gas permeability and promote selective separations, the synergistic combination between polymer and inorganic materials remains as a big challenge. The addition of silica particles through sol-gel method has offered strong interactions between particles and several polymer matrix and the improvement on the thermal and morphological properties of composite membranes have occurred. (Davoodi *et al*., 2016; Ghadimi *et al*., 2014). These improvements suppose that better gas separation properties can be reached, making

a prosperous methodology for composite membrane fabrication. In fact, studies in this field have shown the increase on CO_2 permselectivity properties in silica-containing composite membranes (Rafiq *et al*., 2012).

In this work, the preparation of composite membranes based on polysulfone and silica particles synthesized in-situ by sol-gel method is reported. In order to study the effect of an aminosilane on the formation of silica particles by sol-gel, a comparative study dependent on the concentration and type of inorganic polymerization precursor was developed. The morphological, structural and thermal properties of the resulting polysulfone-silica composite membranes were investigated. In order to evaluate the potential application of these membranes in gas separation, an initial study of the CO_2/CH_4 permeation properties of some membranes was carried out.

2 Materials and methods

2.1 Materials

Tetraethylorthosilicate (TEOS, Aldrich 98%) and 3-aminopropyltriethoxysilane (APTES, Aldrich 97%) were used as silica precursors. Polysulfone (Psu) UDEL-1700 was obtained from Solvay Advanced Polymers. Chloroform and ethanol used as solvent were purchased from J.T. Baker (ACS reagent grade, 99.95%). Deionized water was obtained from a system of four ionic interchange columns (Cole-Parmer Instruments) and hydrochloric acid (J.T. Baker, 36.5-38%) was used to prepare the hydrolyzing solution.

2.2 Preparation of polysulfone-silica composite membranes

In order to prepare the Psu-silica composite membranes, different content of silica precursor was assessed: TEOS, APTES and a mixture of both (TEOS/APTES 75/25 wt/wt) at 10 wt% (0.24g) and 25 wt% (0.6g) respect to the polymer. Firstly, the silica precursor was diluted in 1 mL of $CHCl_3$ and added dropwise to 14 mL of polysulfone solution in $CHCl_3$ (12 wt%). This solution was stirred at room temperature during 15 min. After that, 0.28 mL of 0.15M HCl aqueous solution diluted in 1 mL of ethanol were added dropwise (Romero *et al*., 2011; Zoppi *et al*., 2000) The resulting solution was kept under reflux and magnetic stirring. A white suspension of polysulfone-silica was obtained after 20 h of reaction. For comparison, pure silica particles were prepared under similar reaction conditions. In order to prepare the composite membranes, 3 mL of the white suspension of polysulfone-silica were poured into a glass mold of 5 x 5 cm covered with a funnel to allow the slow solvent evaporation at room temperature overnight. The flat composite membrane was slowly dried in a vacuum oven to remove the residual solvent at 40, 80, 110 and 150 °C in intervals of 8 h each temperature.

2.3 Characterization

The cross-section images of composite membranes were obtained by scanning electron microscopy using a JEOL JSM-7401F microscope. The composite membranes were fractured in liquid nitrogen and coated with silver. An elemental mapping and semiquantitative analysis of composite membranes were obtained by energy dispersive X-ray spectroscopy. Attenuated Total Reflectance Fourier Transform Infrared spectra of composite membranes were acquired using a Nicolet Magna 550 spectrometer in a range of 4000 to 700 cm^{-1}. The pure silica samples were mixed with KBr to prepare pellets for the analysis. Thermogravimetric analysis of composite membranes was performed with a Labsys Evo 1600 thermoanalyst Setaram. The measurements were carried out at heating rate of 10 °C/min under nitrogen flow until 600 °C and then with oxygen flow until 800 °C. Differential scanning calorimetry thermograms were obtained by means of TA Instruments 2920 Modulated MDSC from 0 to 225 °C using a heating rate of 10 °C/min under nitrogen flow. The glass transition temperature (T_g) values were obtained from the second heating cycle. X-ray diffraction patterns were obtained with a Siemens D5000 diffractometer with Ni filter operated at 25 kV and 35 mA using CuKα radiation (1.54 Å). The measurements were performed from 2 to 40° of 2θ with a step size of 0.03° and a step time of 8 s.

2.4 Mixed-gas permeation tests

Gas permeability measurements were performed with a specially designated mixed-gas permeation cell. A binary mixture CH_4/CO_2 (95/5 % mol) was assessed. The membrane was mounted in the middle of the permeation cell onto a porous ceramic support separating the upstream chamber and the downstream chamber. The upstream chamber was pressurized

with the gas mixture. Two different pressures in the upstream side were assessed, 50 and 150 psi. Before that, the permeation cell was swept by helium (He) for baseline. A gas chromatographer 490 Micro GC was used to analyze the permeate gas composition at downstream chamber. A helium stream was used as carrier gas on the permeate side with a flow rate of 10 ml/min. During the test, the temperature on the permeation cell was kept at 35°C. The permeability (P) for each gas was calculated with Eq. (1):

$$P = \frac{\delta J}{p_1 - p_0} \tag{1}$$

Where δ (cm) is the membrane thickness (98μm) measured with a Mitutoyo digital indicator, J (cm^3/cm^2 s) is the penetrant flux, p1 (cmHg) is the partial pressure of the gas in the upstream side and p0 (cmHg) is the partial pressure of the gas in the downstream side. The selectivity (S) was calculated with the CO_2 permeability divided by the CH_4 permeability following Eq. (2):

$$S = \frac{P_{CO_2}}{P_{CH_4}} \tag{2}$$

3 Results and discussion

Composite membranes from silica particles synthesized via sol-gel method into polysulfone matrix were prepared. The effect of type and content of silica precursor on the morphological and physicochemical properties of polysulfone-silica composite membranes was studied.

3.1 SEM analysis

Morphological characterization of composite membranes prepared with TEOS, APTES and mixture of TEOS/APTES was carried out by SEM (Fig. 1). A poor content of silica particles in the composite membranes prepared with TEOS as silica precursor at both 10 and 25 wt% can be appreciated in Fig. 1(a) and (b). This could be due to the difficulties to keep the silica particles in suspension into the liquid polysulfone phase. As a result, only few silica particles could be transferred to the membrane during the casting process. In contrast, a different behavior was appreciated in the composite membranes prepared from TEOS and APTES mixture at 10 wt%. In Fig. 1(c) can be seen the presence of submicrometric silica particles accumulated into polymer cavities. The population of silica particles significantly increased when TEOS/APTES content was increased to 25 wt%. The particle size in the submicrometric range was kept under this reaction conditions as can be seen in the SEM image on Fig. 1(d). It suggests that the addition of APTES favored the dispersion of silica particles into the polymeric solution leading the formation of composite membranes with higher content of silica particles. The formation of silica particles homogeneously distributed throughout the polysulfone matrix was also appreciated when a 10 wt% of APTES was used as silica source as can be seen in the SEM image of the composite membrane in Fig. 1(e). However, interfacial voids between silica particles and polymeric matrix were clearly observed. This morphology commonly called as “sieve in a cage" has been reported as indicative of poor contact between phases (Gorgojo *et al*., 2008; Vinoba *et al*., 2017). Increasing APTES content to 25 wt% allowed the formation of a composite membrane without interfacial voids and well-dispersed inorganic phase (Fig. 1(f)). These SEM results suggested that the use of a greater amount of amino-containing silica source improved the adhesion between amino silica particles and polymer matrix. In addition, it was found that the higher APTES content in the initial gel composition, the larger silica particle size. In SEM images it can be distinguished that the particles size of sample prepared with APTES 25 wt% ranging 2-5 μm while sample with APTES 10 wt% showed particle size less than 1 μm. This particle size variation is attributed to the amino groups in APTES, which increase the hydrolysis rate of the inorganic precursor and promote the particle growth (Rahman *et al*., 2012). The chemical analysis and the elemental mapping for Si directly on the cross-section SEM image of Psu-APTES 25 wt% composite membrane were performed by energy dispersive X-ray spectroscopy (Fig. 2). The EDX spectrum on Fig. 2(a) showed the elements present in the polymeric matrix of polysulfone such as C and S. The elements Si and N were detected due to the presence of the silica particles containing amino groups. In addition, the element O was detected because was present in both polymeric matrix and silica particles. The distribution mapping of Si is displayed in Fig. 2(b). The mapped image in green color represents the scanned area of membrane containing Si and suggesting the location of silica particles.

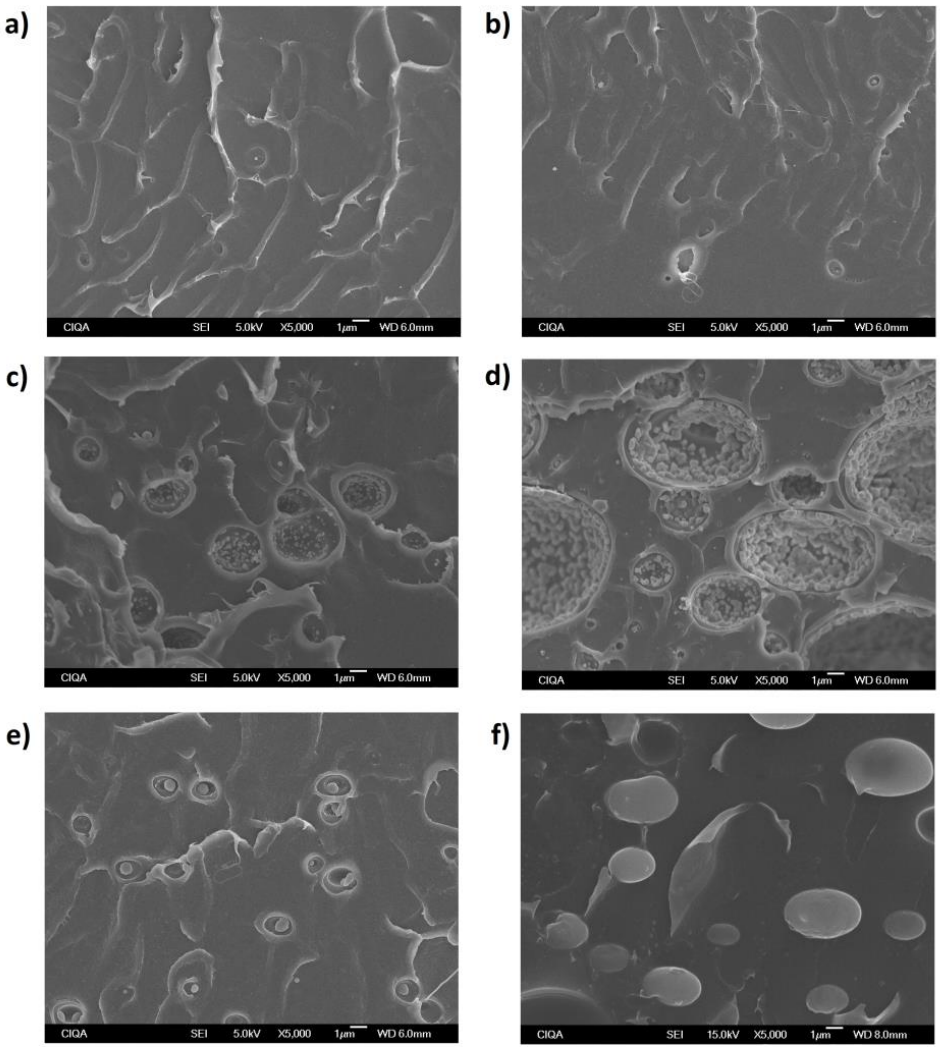

Fig. 1 Cross section images of composite membranes obtained by SEM. a) Psu-TEOS 10%, b) Psu-TEOS 25%, c) Psu-TEOS/APTES 10%, d) Psu-TEOS/APTES 25%, e) Psu-APTES 10%, f) Psu-APTES 25%.

In fact, the distribution of these zones in green matched well with the location of the silica particles dispersed into the composite membrane as is shown in the X-ray elemental mapping overlapped on the respective SEM image in Fig. 2(c). This analysis could indicate that all Si source was stayed in the silica particles formed during the sol-gel process.

3.2 FTIR spectroscopy

The spectra of polysulfone and composite membranes are given in Fig. 3. The spectrum of polysulfone membrane showed two peaks at 1585 and 1487 cm^{-1} related to the C-C and C-H aromatic vibration, respectively. Other important peaks at 1241, 1146 and 693 cm^{-1} associated to the C-O, S=O and C-S stretching vibration, respectively, were observed. In addition to the peaks corresponding to the polysulfone matrix, the spectra of the Psu-APTES and Psu-TEOS/APTES composite membranes exhibited a slight widening of the low intensity peak at 1018 cm^{-1} that could be associated to the Si-O-Si vibration of silica particles. Particularly, in the composite membranes derived from APTES can be distinguished the N-H flexion vibration at 1670 cm^{-1} (Bilalis *et al*., 2016) whose intensity increased with the increment of APTES content in the initial composition.

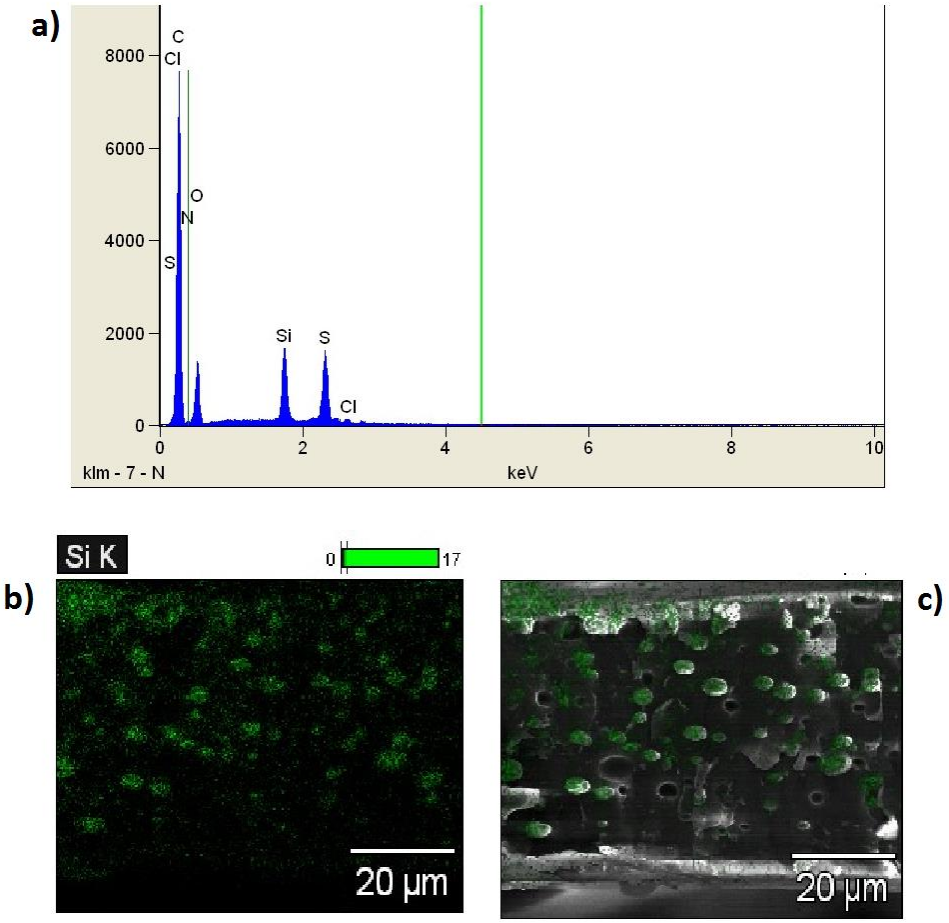

Fig. 2 Psu-APTES 25% composite membrane a) EDX spectrum, b) Elemental mapping for Si, c) Si-mapping overlapped on the SEM image.

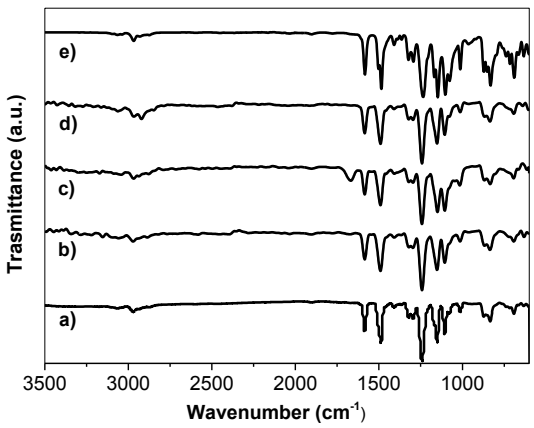

Fig. 3 FTIR spectra of polymeric and composite membranes: a) Psu, b) Psu-APTES 10%, c) Psu-APTES 25%, d) Psu-TEOS/APTES 10%, e) Psu-TEOS/APTES 25%.

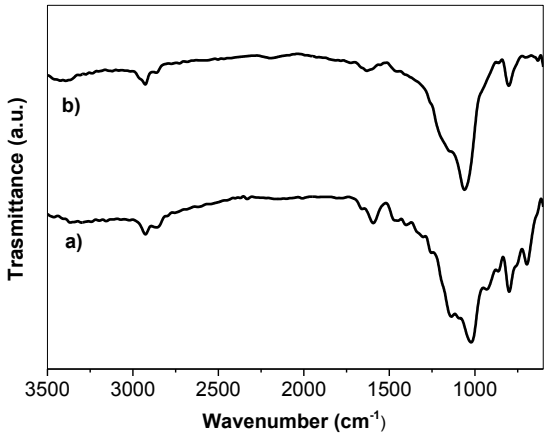

Fig. 4 FTIR specta of silica particles synthesized from a) APTES and b) TEOS/APTES mixture.

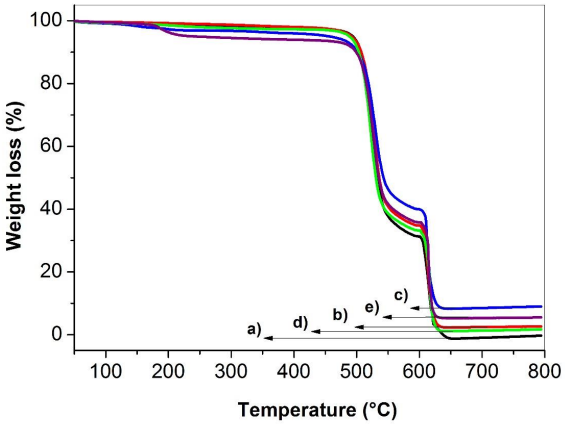

Fig. 5 TGA thermograms of polymeric and composite membranes. a) Psu, b) Psu-APTES 10%, c) Psu-APTES 25%, d) Psu-TEOS/APTES 10%, e) Psu-TEOS/APTES 25%.

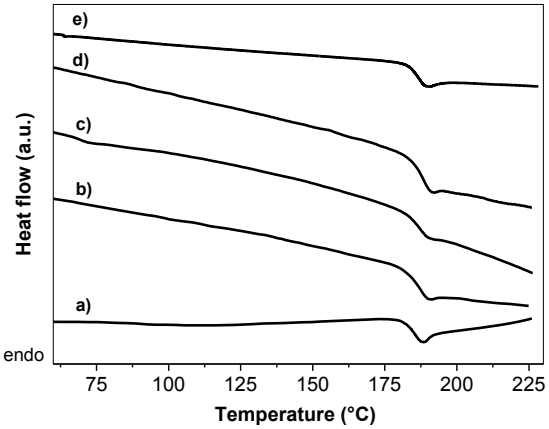

Fig. 6 DSC thermograms of polymeric and composite membranes. a) Psu, b) Psu-APTES 10%, c) Psu-APTES 25%, d) Psu-TEOS/APTES 10%, e) Psu-TEOS/APTES 25%.

As it was expected, the Si-O-Si asymmetric stretching peak at 1020 and 1055 cm^{-1}, symmetric stretching peak at 800 and 802 cm^{-1} and N-H flexion vibration peak at 1600 and 1630 cm^{-1} were clearly observed in the spectra of amorphous silica particles that were synthesized for comparison from APTES and mixture of TEOS/APTES, respectively (Fig. 4). Additionally, the bands of asymmetric -CH_2-, symmetric -CH_3 and -CH_2- stretching vibrations from the aminopropyl group were observed at 2930 and 2850 cm^{-1}, respectively.

3.3 Thermal analysis

TGA thermograms of composite membranes and polymeric membrane showed two-steps degradation process as is appreciated in Fig. 5. Psu membrane showed good thermal stability whose main weight loss about 500 °C was attributed to the thermal decomposition of polymeric chains and sulfone rupture. The second weight loss associated to the carbonization phase of residue started at 620 °C (Zhu *et al*., 2014). Composite membranes synthesized at different content of either APTES or TEOS/APTES mixture showed analogous thermal behavior to the Psu membrane. Two main weight losses attributed to the polymer matrix were appreciated at 500 and 620 °C. In addition, the samples synthesized from 25% both APTES and TEOS/APTES showed a slight weight loss about 200°C suggesting the presence of residual solvent occluded into the membrane.

These results indicated that the thermal stability of composite membranes was maintained despite of amino-functionalized silica particles. As was expected, the remaining weight loss of Psu membrane approached to zero at 800 °C. On the other hand, the remaining weight loss of composite membranes would be related to the weight loading of silica particles. The calculated remaining weight for all composite membranes was less than the expected theoretical weight percentage. This behavior could be associated to the accumulation of silica particles in certain areas of the membrane and the wide particle size distribution as could be appreciated in the SEM images. DSC curves of polysulfone and composite membranes prepared with different content of APTES are shown in Fig. 6. An endothermic peak located at 183 °C was observed for the pure polymeric membrane which was due to the glass transition temperature (T_g) of polysulfone. A slight increase of T_g was detected for composites membranes, recording values at 186 °C. This suggests that the movement restriction of the polymer chains attributed to interactions (promoted by amino groups) between silica particles and polysulfone matrix was present (Zornoza *et al*., 2011).

3.4 XRD analysis

The XRD patterns of silica particles synthesized from different precursors, the polymeric and composite membranes are given in Fig. 7. The XRD pattern of Psu membrane showed a broad peak centered at 18° of 2θ which corresponds to the d-spacing of 4.92 Å

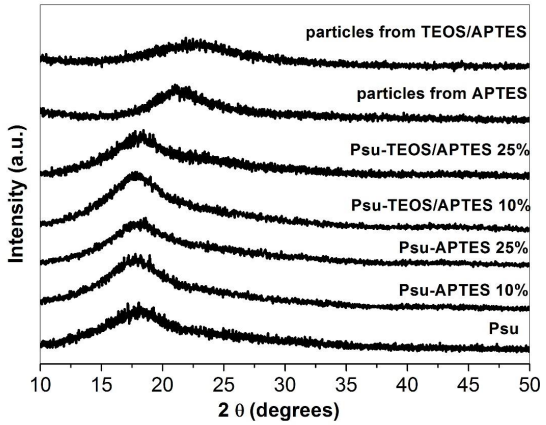

Fig. 7. XRD patterns of silica particles, polymeric and composite membranes.

and it is associated to the amorphous arrangement of the polymeric chains (Gaur *et al*., 2013). On the other hand, the silica particles synthesized from APTES and TEOS/APTES mixture also showed an amorphous behavior (Chen *et al*., 2009). A broad peak centered at 21° and 27° of 2θ was appreciated for the silica particles synthesized from APTES and TEOS/APTES mixture, respectively. Particularly, in composite membrane it could be appreciated a slight shift of the peak to 17.84° of 2θ when the content of silica APTES precursor was 25wt%, indicating an increase on the distance between polysulfone chains (d-spacing) and suggesting the increment in free volume. Moreover, the slight decrease in the intensity of this peak is an indicative of the interruption on the polymer chains packing due to the presence of silica particles (Rafiq *et al*., 2012; Zhao *et al*., 2012; Wang *et al*., 2015). Like, the broad peak from silica particles was possibly overlapped by the peak of polysulfone.

3.5 Gas separation measurements

In order to know the gas separation performance of these membranes, a preliminary study using a CO_2/CH_4 mixture at different upstream pressures was carried out. The gas permeability studies on composite membranes derived from APTES were carried out due to the homogenous distribution and no agglomerated particles were appreciated. Psu-APTES 10% failed in the gas separation performance because extremely high permeability values for both CO_2 and CH_4 were calculated. In this case, it is possible that the interfacial voids between particles and polymer allowed no selective pathway for both CH_4 and CO_2 gases (Aroon *et al*., 2010; Pechar *et al*., 2006). In this context, Martin-Gil *et al*. (2017) reported the drop of CO_2/CH_4 separation factor from 32.6 to 27.5 for polyimide-ETS-10 as a result of defects derived of the highest particle loading.

The gas permeation and selectivity for Psu membrane and composite membrane Psu-APTES 25% obtained at different upstream pressures are given in Table 1. The solution-diffusion mechanism explains the gas permeation through polymeric membranes (Ismail *et al*., 2002), being the solubility the main criterion in such mechanism. As was expected, CO_2 permeability higher than CH_4 permeability was obtained due to the higher CO_2 condensability. The solubility depends on the gas condensability, thus, higher condensability would suppose higher permeability. Considering the test conditions assessed in this work, the CO_2 and CH_4 permeability for the Psu membrane at 50 psi were 4.8 and 0.2 barrier, respectively and the selectivity was 24. Improved CO_2 permeability properties were exhibited by the composite membrane Psu-APTES 25% achieving 20.5 barrer.

Based on free-volume increase mechanism, this behavior could be related to the disruption in the polymer-chain packing by particles, similar to Rafiq *et al.´*s. (2012) report. They reported that CO_2 permeance increased from 73.7 GPU to 95.7 GPU with the addition of silica loading. Other researchers (Mohagheghian *et al*., 2014; Andrady *et al*., 2004) like Cong *et al*. (2007) have also reported significantly improvement in composite membrane performance, achieving CO_2 permeability of 177 barrer which represents about 2.2 times of that pure polymer

Table 1. CO_2/CH_4 permeation properties of polymeric and composite membranes.

Membrane	Upstream pressure (psi)	CO_2 Permeability (Barrer)	CH_4 Permeability (Barrer)	Ideal selectivity
Psu	50	4.8	0.2	24.0
	150	2.9	0.1	29.0
Psu-APTES	50	20.5	1.4	14.6
25%	150	14.0	0.5	28.0

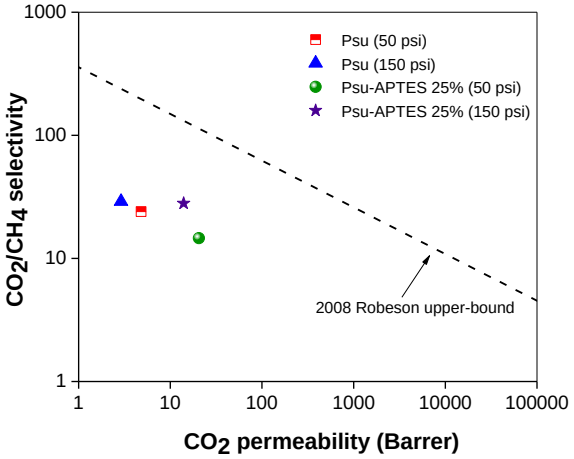

Fig. 8 CO_2/CH_4 ideal selectivity against CO_2 permeability of polymeric and composite membranes.

membrane. In addition, NH_2 group in silica particles can improve the solubility of CO_2 within the membrane increasing the permeability by means of the formation of Langmuir-sites as have been suggested by several authors (Miki *et al*., 2013; Basu *et al*., 2010). Kim *et al*. (2008) reported the addition of 20% of amino-modified silica in composite membranes enhanced the CO_2/CH_4 ideal selectivity from 23 to 28 regarding to that containing no-modified silica particles.

On the other hand, increasing the upstream pressure to 150 psi, the CO_2 and CH_4 permeability values for both polymeric and composite membranes decreased, indicating no plasticization of polysulfone took place (Visser *et al*., 2008). This suppose that a competing effect of compression on the polymer matrix at higher pressure could be reducing the free volume and the diffusion of penetrants, resulting on the reduction of the permeability values (Merkel *et al*., 2000). The trade-off between permeability and selectivity remains as the main challenge in membrane-based gas separation (Cong *et al*., 2007). In Fig. 8 it can be seen the tendency of the CO_2 permeability regarding CO_2/CH_4 selectivity of membranes evaluated in this work and the comparative with the upper bound correlation for CO_2/CH_4 separation reported by Robeson (2008). In this context, it is important to note that in this work, the enhancement of CO_2 permeability and CO_2/CH_4 selectivity on composite membranes were achieved in comparison to those showed for the pure polymeric membrane even at the highest upstream pressure. Increases in CO_2/CH_4 selectivity regarding upstream pressure increase was also been appreciated in composite membranes by Sridhar *et al*. (2008), showing 15.2 at 10 psi and 17.4 at 30 psi. The results here discussed indicated that silica particles containing amino groups and prepared under the sol-gel method can improve the permeation properties and maintain good selectivity of membranes based on polysulfone.

Conclusions

Composite membranes based on polysulfone matrix and silica particles synthesized from APTES and TEOS/APTES mixture were successfully prepared by the sol-gel method under acidic conditions. The morphological, thermal and structural properties of composite membranes were studied by SEM, DSC, TGA, FTIR, and XRD. It was possible to prepare composite membranes up to 25 wt% of organoaminosilane as silica precursor. Different morphological properties dependent on the silica source were exhibited. Silica particles in the submicrometric range were obtained from TEOS/APTES mixtures. On the other hand, the use of APTES produced larger silica particles whose particle size was dependent on the initial silica source concentration. Improved particle-polymer adhesion was achieved using APTES as an inorganic precursor at 25 wt% because of defect-free composite membrane was appreciated. These silica particles showed the largest particle size between 2 to 5 μm. No significant effect of silica particles on the structural and thermal properties of composite membranes was detected. Enhancement on the CO_2 permeability and CO_2/CH_4 selectivity were achieved. The mixed-gas permeation properties demonstrated the potential application of the composite membranes based on polysulfone and silica particles synthesized from APTES as membrane for separation of CO_2 from CH_4.

Nomenclature

P	permeability (Barrer)
δ	membrane thickness (cm)
J	penetrant flux (cm^3/cm^2s)
p_1	upstream partial pressure (cmHg)
p_2	downstream partial pressure (cmHg)
S	selectivity
PCO_2	CO_2 permeability
PCH_4	CH_4 permeability

Acknowledgments

Authors are grateful to CIQA (project 6163) and CONACYT-Sener-Hydrocarbons Found (project 267962) for the financial resources. G Castruita-de León and H. I. Meléndez-Ortiz are grateful to Cátedras-CONACYT. We are also thanking to Jesus A. Cepeda, Julieta Sanchez and Guadalupe Mendez for their support for SEM, FTIR and DSC analyses, respectively, and Bertha A. Puente for her technical assistance.

References

Andrady, A.L., Merkel, T.C., Toy, L.G. (2004). Effect of particle size on gas permeability of filled superglassy polymers. *Macromolecules 37*, 4329-4331.

Armstrong, G., Thornton, R., Ryan, M.P., Laffir, F., Russel, R.J., Bala, T., Keely, C., Babu, R. (2012). Formulation of epoxy-polyester powder coatings containing silver-modified nanoclays and evaluation of their antimicrobial properties. *Polymer Bulletin 68*, 1951-1963.

Aroon, M.A., Ismail, A.F., Matsuura, T., Montazer-Rahmati, M.M. (2010). Performance studies of mixed matrix membranes for gas separation: A review. *Separation and Purification Technology 75*, 229-242.

Babanzadeh, S., Mehdipour-Ataei, S., Mahjoub, A.R. (2012). Preparation and characterization of novel polyimide/SiO_2 nano-hybrid films by *in situ* polymerization. *Journal of Inorganic and Organometallic Polymer 22*, 1404-1412.

Basu, S., Khan, AL., Cano-Odena, A., Liu, C., Vankelecom, I.F.J. (2010). Membrane-based technologies for biogas separations. *Chemical Society Reviews 39*, 750-768.

Bilalis, P., Tziveleka, L.A., Varlas, S., Iatrou, H. (2016). pH-Sensitive nanogates based on poly(L-histidine) for controlled drug release from mesoporous silica nanoparticles. *Polymer Chemistry 7*, 1475-1485.

Castruita-de León, G., Perera-Mercado, Y.A., García-Cerda, L.A., Mercado-Silva, J.A., Meléndez-Ortiz, H.I., Olivares-Maldonado Y., Alvarez-Contreras, L. (2015). Synthesis of amino-functionalized MCM-48 silica via direct co-condensation at room temperature. *Microporous and Mesoporous Materials 204*, 156-162.

Chen, S., Hayakawa, S., Shirosaki, Y., Fujii, E., Kawabata, K., Tsuru, K., Osaka, A. (2009). Sol-Gel synthesis and microstructure analysis of amino-modified hybrid silica nanoparticles from aminopropyltriethoxysilane and tetraethoxysilane. *Journal of American Ceramic Society 92*, 2074-2082.

Chew, T.L., Ahmad, A.I., Bathia, S. (2010). Ordered mesoporous silica (OMS) as an adsorbent and membrane for separation of carbon dioxide (CO_2). *Advances in Colloid Interface Science 153*, 43-57.

Chung, T.S., Jiang, L.Y., Li, Y., Kulprathipanja, S. (2007). Mixed matrix membranes (MMM) comprising organic polymers with dispersed inorganic fillers for gas separation. *Progress in Polymer Science 32*, 483-507.

Cong, H., Hu, X., Radosz, M., Shen, Y. (2007). Brominated poly(2,6-diphenyl-1,4-phenylene oxide) and its silica nanocomposite membranes for gas separation. *Industrial and Engineering Chemistry Research 46*, 2567-2575.

Davoodi, S.M., Sadeghi, M., Naghsh, M., Moheb, A. (2016). Olefin-paraffin separation performance of polyimide Matrimid/silica nanocomposite membranes. *RSC Advances 6*, 23746-23759.

Gaur, M.S., Singh, P.K., Saruchi, Chauhan, R.S. (2013). Structural and thermal properties of polysulfone-ZnO nanocomposites. *Journal of Thermal Analysis and Calorimetry 111*, 743-751.

Ghadami, A., Mohammadi, T., Kasiri, N. (2014). A novel chemical surface modification for the fabrication of PEBA/SiO_2 nanocomposite membranes to separate CO_2 from syngas and natural gas streams. *Industrial and Engineering Chemistry Research 53*, 17476-17486.

Gil, M., Tiscornia, I., de la Iglesia, O., Mallada, R., Santamaría, J. (2011). Monoamine-grafted MCM-41: An efficient material for CO_2 removal at low partial pressures. *Chemical Engineering Journal 175*, 291-297.

Gorgojo, P., Uriel, S., Téllez, C., Coronas, J. (2008). Development of mixed matrix membranes based on zeolite Nu-6(2) for gas separation. *Microporous and Mesoporous Materials 115*, 85-92.

Hasebe, S., Aoyama, S., Tanaka, M., Kawakami, H. (2017). CO_2 separation of polymer membranes containing silica nanoparticles with gas permeable nano-space. *Journal of Membrane Science 536*, 148-155.

Hasik, M., Turek, W., Nyczyk, A., Stochmal, E., Bernasik, A., Sniechota, A., Soltysek, A. (2009). Application of conjugated polymer-platinum group metal composites as heterogeneous catalysts. *Catalysis Letter 127*, 304-311.

Ismail, A.F., Lorna, W. (2002). Penetrant-induced plasticization phenomenon in glassy polymers for gas separation. *Separation and Purification Technology 27*, 173-194.

Jomekian, A., Pakizeh, M., Shafiee, A.R., Mansoori, S.A.A. (2011). Fabrication or preparation and characterization of new modified MCM-41/Psf nanocomposites membrane coated by PDMS. *Separation and Purification Technology 80*, 556-565.

Kang, N.K., Jun, T.S., La, D.D., Oh, J.H., Cho, Y.W., Kim, Y.S. (2010). Evaluation of the limit-of-detection capability of carbon black-polymer composite sensors for volatile breath biomarkers. *Sensors and Actuators B 147*, 55-60.

Khosravi, A., Sadhegi, M., Banadkohi, H.Z., Talakesh, M.M. (2014). Polyurethane-silica nanocomposite membranes for separation of propane/methane and ethane/methane. *Industrial and Engineering Chemistry Research 53*, 2011-2021.

Kim, J.H., Lee, Y.M. (2001). Gas permeation properties of poly(amide-6-b-ethylene oxide)-silica hybrid membranes. *Journal of Membrane Science 193*, 209-225.

Kim, S., Marand, E. (2008). High permeability nano-composite membranes based on mesoporous MCM-41 nanoparticles in polysulfone matrix. *Microporous and Mesoporous Materials 114*, 129-136.

Lua, A.C., Shen, Y. (2013). Preparation and characterization of polyimide-silica composite membranes and their derived carbon-silica composite membranes for gas separation. *Chemical Engineering Journal 220*, 441-451.

Mahajan, R., Burns, R., Schaeffer, M., Koros, W.J. (2002). Challenges in forming successful mixed matrix membranes with rigid polymeric materials. *Journal of Applied Polymer Science 86*, 881-890.

Merkel, T.C., Bondar, V.I., Nagai, K. Freeman, B.D., Pinnau, I. (2000). Gas sorption, diffusion, and permeation in poly(dimethylsiloxane). *Journal of Polymer Science B 38*, 415-434.

Martin-Gil, V, López, A, Hrabanek, P., Mallada, R., Vankelecom, I.F.J., Fila, (2017). Study of different titanosilicate (TS-1 and ETS-10) as fillers for mixed matrix membranes for CO_2/CH_4 gas separation applications. *Journal of Membrane Science 523*, 24-35.

Miki, M., Houriuchi, H., Yamada, Y. (2013). Synthesis and gas transport properties of hyperbranched polyimide-silica hybrid/composite membranes. *Polymers 5*, 1362-1379.

Mohagheghian, M., Sadeghi, M., Chenar, P.M., Naghsh, M. (2014). Gas separation properties of polyvinylchloride (PVC)-silica nanocomposite membrane. *Korean Journal of Chemical Engineering 31*, 2041-2050.

Naghsh, M., Moheb, A., Chenar, M.P., Mohagheghian, M. (2012). Separation of ethylene/ethane and propylene/propane by cellulose acetate-silica nanocomposite membranes. *Journal of Membrane Science 423-424*, 97-106.

Pechar, T.W., Kim, S., Vaughan, B., Marand, E., Tsapatsis, M., Jeong, H.K., Cornelius, C.J. (2006). Fabrication and characterization of polyimide-zeolite L mixed matrix membranes for gas separation. *Journal of Membrane Science 277*, 195-202.

Pérez-Escobedo, A., Díaz-Flores, P.E., Rangel-Méndez, J.R. Cerino-Corova, F.J., V.M. Ovando-Medina, Alcalá-Jáuregui, J.A. (2016). Fluoride adsorption capacity of composite based on chitosan-zeolite-algae. *Revista Mexicana de Ingeniería Química 15*, 139-147.

Rafiq, S., Man, Z., Maulud, A., Muhammad, N., Maitra, S. (2012). Separation of CO_2 from CH_4 using polysulfone/polyimide silica nanocomposite membranes. *Separation and Purification Technology 90*, 162-172.

Rahman, I.A., Padavettan, V. (2012). Synthesis of silica nanoparticles by sol-gel: size-dependent properties, surface modification, and applications in silica-polymer nanocomposites-A review. *Journal of Nanomaterials 2012*, 1-15.

Robeson, L.M. (2008). The upper bound revisited. *Journal of Membrane Science 320*, 390-400.

Romero, A.I., Parentis M.L., Habert A.C., Gonzo E.E. (2011). Synthesis of polyetherimide/silica hybrid membranes by sol-gel process: Influence of the reaction conditions on the membrane properties. *Journal of Materials Science 46*, 4701-4709.

Romero, I., Parentis, M.L., Sham, E.L., Gonzo E.E. (2013). Influence of silica and coupling agent loading on thermal, morphological and mechanical properties of hybrid membranes. *Polymer Bulletin 70*, 2305-2317.

Sadeghi, M., Semsarzadeh, M.A., Barikani, M., Chenar, M.P. (2011). Gas separation properties of polyether-based polurethane-silica nanocomposites membranes. *Journal of Membrane Science 376*, 188-195.

Sánchez-Ruiz, A., Robles-Guitiérrez I, Espejel-Ayala F. (2018). Preparation of zeolitic material using natural clinoptilolite for CO_2 capture. *Revista Mexicana de Ingeniería Química 17*, 573-585.

Sridhar, S., Smitha, B., Suryamurali, R., Aminabhavi, T.M. (2008). Synthesis, characterization and gas permeability of an activated carbon-loaded PEBAX 2533 membrane. *Designed Monomers and Polymers Journal 11*, 17-27.

Starlet Thanjam, I., Francklin Philips, M., Lee, K.P., Gopalan, A. (2012). Preparation of poly(4-aminodiphenylamine)/silver nanoparticles composites and catalysis. *Journal of Materials Science: Materials in Electronics 23*, 807-810.

Torrey, J.D., Bordia, R.K. (2008). Mechanical properties of polymer-derived ceramic composite coatings on steel. *Journal of the European Ceramic Society 28*, 253-257.

Vallés-Lluch, A., Costa, E., Gallego Ferrer, G., Monleón Pradas, M., Salmerón-Sánchez, M. (2010). Structure and biological response of polymer/silica nanocomposites prepared by sol-gel technique. *Composites Science and Technology 70*, 1789-1795.

Vinoba, M., Bhagiyalakshmi, Alqaheem, Y., Alomair, A.A., Pérez, A., Rana, M.S. (2017). Recent progress of fillers in mixed matrix membranes for CO_2 separation: A review. *Separation and Purification Technology 188*, 431-450.

Visser, T., Wessling, M. (2008). Auto and mutual platicization in single and mixed gas C_3 transport through Matrimid-based hollow fiber membranes. *Journal of Membrane Science 312*, 84-96.

Wang, M., Wang, Z., Li, N., Liao, J., Zhao, S., Wang, J., Wang, S. (2015). Relationship between polymer-filler interfaces in separation layers and gas transport properties of mixed matrix composite membranes. *Journal of Membrane Science 495*, 252-268.

Wei, J., Li, Y., Lau, K.T. (2007). Preparation and characterization of a nano-apatite/polyamide6 bioactive composite. *Composites: Part B 38*, 301-305.

Wu, H,, Tang, B., Wu, P. (2013). Optimizing polyamide thin film composite membrane covalently bonded with modified mesoporous silica nanoparticles. *Journal of Membrane Science 428*, 341-348.

Xu, Z.L., Yu, L.Y., Han, L.F. (2009). Polymer-inorganic particles composite membranes: a brief overview. *Frontiers of Chemical Engineering in China 3*, 318-329.

Zarazua-Aguilar, Y., Paredes-Carrera, S.P., Sánchez-Ochoa, J.C., Avendaño-Gómez, J.R., Flores-Valle, S.O. (2017). Influence of microwave/ultrasound irradiation on the sol-gel synthesis of titanium nanoparticles for application in photocatalysis. *Revista Mexicana de Ingeniería Química 16*, 899-909.

Zhao, J., Wang, Z., Wang, J., Wang, S. (2012). High-performance membranes comprising polyaniline nanoparticles incorporated into polyvinylamine matrix for CO_2/N_2 separation.

Journal of Membrane Science 403-404, 203-215.

Zeng, W., Zhang, M.Q., Rong, M.Z., Zheng, Q. (2007). Conductive polymer composites as gas sensors with size-related molecular discrimination capability. *Sensors and Actuators B 124*, 118-126.

Zhu, F.L., Feng, Q.Q., Xin, Q., Zhou, Y. (2014). Thermal degradation process of polysulfone aramid fiber. *Thermal Science 18*, 1637-1641.

Zhuang, G.L., Tseng, H.H., Wey, M.Y. (2014). Preparation of PPO-silica mixed matrix membranes by in-situ sol-gel method for H_2/CO_2 separation. *International Journal of Hydrogen Energy 39*, 17178-17190.

Zoppi, R.A., des Neves S., Nunes S.P. (2000). Hybrid fulms of poly(ethylene oxide-b-amide-6) containing sol-gel silicon or titanium oxide as inorganic fillers: effect of morphology and mechanical properties on gas permeability. *Polymer 41*, 5461-5470.

Zornoza, B., Téllez, C., Coronas, J. (2011). Mixed matrix membranes comprising glassy polymers and dispersed mesoporous silica spheres for gas separation. *Journal of Membrane Science 368*, 100-109.